Molecular and Electronic Structure and Gas-Phase Pyrolytic Generation of 7,7′-Dioxasesquinorbornenes

Ivana Antol[a], Mirjana Eckert-Maksić*[a], Davor Margetić[‡][a], Zvonimir B. Maksić[a], Klaus Kowski[b], and Paul Rademacher[b]

Division of Organic Chemistry and Biochemistry, "Rudjer Boskovic" Institute[a],
Bijenicka cesta 54, 10001 Zagreb, Croatia
E-mail: mmaksic@emma.irb.hr

Institut für Organische Chemie der Universität Essen[b],
D-45117 Essen, Germany

Received February 3, 1998

Keywords: Pyramidalization / Ab initio calculations / DFT calculations / Pyrolysis / Photoelectron spectroscopy

Structural and photoelectron spectroscopic (PES) features of 7,7′-dioxa analogs of *syn*- (*syn*-**2**) and *anti*-sesquinorbornenes (*anti*-**2**) are investigated. It is shown that the B3LYP/6-31G* and B3PW91/6-31G* DFT methods are well-suited for studying the geometrical properties of large organic molecules containing nonplanar double bonds, as is evident from comparisons with MP2/6-31G* results and the available neutron diffraction and X-ray data. It is also shown that the *anti* isomer is less stable than the *syn* isomer of **2**, in accordance with the stability ordering of *syn*-**1** and *anti*-**1**. Finally, PES evidence for the formation of *anti*-**2** upon pyrolytic decomposition of the corresponding β-lactone is given and discussed.

Introduction

syn- (*syn*-**1**) and *anti*-sesquinorbornenes (*anti*-**1**) have been the subject of great interest, both experimentally and theoretically, since their syntheses in the early eighties.[1] Various aspects of their physicochemical properties have been analysed, with particular emphasis on pyramidalization of the olefinic carbon atoms and the resulting nonplanarity of the central double bond in the *syn*-sesquinorbornene framework.[2][3][4][5] An interesting question related to this issue concerns the influence of heteroatoms on the extent of double bond folding, which has consequences regarding the chemical reactivity.[2][6] An illustrative example is provided by comparing the different reactivities of *syn*-benzosesquinorbornene (**3**) and 1,2,3,4,9,10-hexahydro-9,10-*exo*-epoxy-1,4-*exo*-methanoanthracene (**4**) towards the addition of dichlorocarbene. In the case of **3**, treatment with dichlorocarbene for 24 h leads to no reaction at all, whereas treatment of **4** under similar conditions results in complete reaction within 12 h with formation of the dichlorocarbene adduct.[7] On the other hand, the available structural data are not unambiguous with regard to structure/reactivity relationships. For example, the X-ray structure of *syn*-7-oxasesquinorbornene anhydride (**5**)[6a] shows approximately the same degree of double-bond folding as the corresponding hydrocarbon[1a], whereas in **4**[8] a significantly larger deviation from planarity is found. Unfortunately, previous theoretical calculations were performed at a level that was not quite adequate for an accurate description of the structural features of the pyramidalized double bond. This is illustrated by the recent study of Holthausen and Koch[9], who found that a precise description of the double-bond folding in *syn*-sesquinorbornene and related molecules requires inclusion of the valence electron correlation at least at the MP2[10] level of theory. Pursuing our interest in this field, we present here results of MP2 ab initio and DFT[11] calculations using B3LYP[12] and B3PWP91[12a][13] hybrid functionals for the molecules *syn*-**2** and *anti*-**2** (Scheme 1). This is, to the best of our knowledge, the first application of hybrid-based DFT methods in studying geometries of pyramidalized olefins. Hence, in order to provide an insight into their reliability, we also carried out calculations on *exo*,*exo*-2,3-norborna-5-ene dicarboxylic anhydride (**6**)[13], for which accurate neutron diffraction data are available.[14]

Our second task in this study was to examine the possibility of producing *anti*-**2** by flash-vacuum pyrolysis (FVP) of the corresponding β-lactone **7** (Scheme 1) and to explore its electronic structure. This technique has recently been successfully used in our laboratories for the generation of *syn*-**2** and measurement of its He(I)-photoelectron spectrum.[15]

Results and Discussion

Computational Studies

The geometries of *syn*-**2** and *anti*-**2** were calculated using the B3LYP/6-31G* and MP2(fc)/6-31G* theoretical models, whilst calculations on the test molecule **6** were performed at the B3LYP level of theory using the 6-31G* and 6-311G*[16] basis sets, and within the B3PW91/6-31G* framework. The latter approach was also applied in calculating the molecular geometry of *syn*-**2**. We shall commence the discussion by comparing the structural parameters of **6**

[‡] Present address: Centre for Molecular Architecture, Central Queensland University, Rockhampton 4702, Qld., Australia.

Scheme 1

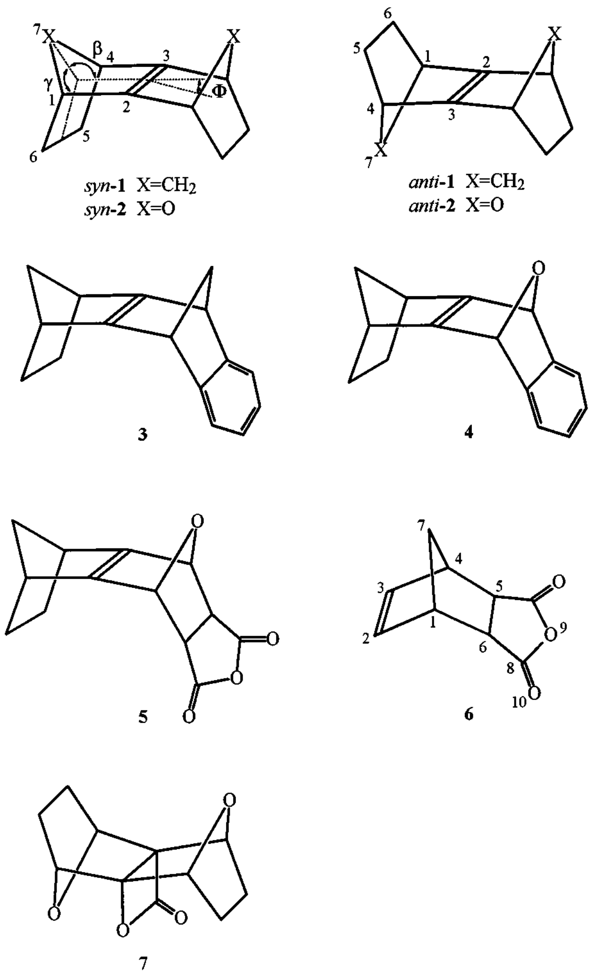

with the previously reported structural data offered by the MP2/6-31G*[9] method and by the neutron-diffraction technique.[14] Selected parameters are listed in Table 1.

Perusal of the tabulated data shows that the calculated structure of **6** is very similar to the previously reported MP2/6-31G* geometry[10], and is in good agreement with the experimental neutron diffraction data.[13] Indeed, most of the calculated bond distances and bond angles appear to be in somewhat better agreement with the experimental findings than the corresponding MP2/6-31G* values. It is also interesting to note that the B3PW91 approach provides the most accurate data, being more precise than the B3LYP model employing the same basis set. A similar trend has been observed previously in the case of MP2 calculations on norbornene.[9] We also note that the increase in flexibility of the basis set on going from 6-31G* to 6-311G* has only a marginal effect on the calculated structural parameters. Focusing on the out-of-plane angle, which, by convention, is defined as the angle between the planes H−C2−C3−H and C1−C2−C3−C4, we observe that the DFT-derived pyramidalization angles (6.2−6.5°) are close to the MP2/6-31G* value (6.8°). Neutron diffraction estimates are 7.3(2)° and 7.5(2)°, implying that all the theoretical results are in reasonable accordance with experiment. We mention in passing that among the applied DFT methods the B3PW91/6-31G* model seems to be a very good compromise between applicability and practicability on the one hand, and reliability on the other. In order to provide additional evidence of the good performance of the DFT-based methods, we calculated the out-of-plane deformation of the double bond in *syn*-sesquinorbornene (*syn*-**1**) within the B3LYP/6-31G* and B3PW91/6-31G* formalisms. Both methods yielded an out-of-plane angle of 15.1°[17], which is ca. 1° smaller than in the MP2/6-31G* optimized structure (16.3°).[9] The corresponding experimental values lie in the range 15−18°, as determined by X-ray studies of various *syn*-sesquinorbornene derivatives.[1][18] Hence, we conclude that the B3LYP/6-31G* and, in particular, the B3PW91/6-31G* DFT method offers a suitable tool for examining the double bond pyramidalization in larger organic systems.

The key bond lengths and angles of the optimized geometries for the title molecules, *syn*-**2** and *anti*-**2**, are collected in Table 2, together with their total energies. Also included are the out-of-plane angles (Φ), and the angles be-

Table 1. Comparison of selected DFT, MP2, and neutron-diffraction structural data for compound **6**[a]

Bond or angle	B3LYP/ 6-31G*	DFT B3LYP/ 6-311G*	B3PW91/ 6-31G*	MP2/[9] 6-31G*	Exp.[14]
C1−C2	1.523	1.522	1.517	1.514	1.519; 1.518
C2−C3	1.341	1.338	1.340	1.349	1.342
C1−C6	1.580	1.579	1.573	1.567	1.572; 1.573
C5−C6	1.542	1.540	1.536	1.535	1.541
C1−C7	1.550	1.549	1.543	1.540	1.544
C8−O9	1.383	1.392	1.387	1.400	1.392; 1.384
C8−O10	1.197	1.190	1.196	1.206	1.193; 1.198
C1−C2−C3	107.6	107.7	107.6	107.4	107.3; 107.7
C1−C7−C4	93.8	93.9	94.0	94.0	94.0
C1−C2−H	124.6	124.7	124.7	124.9	124.8; 124.6
H−C7−H	109.7	109.6	109.8	109.3	109.0
Φ	6.2	6.3	6.5	6.8	7.3(2); 7.5(2)
E_{tot}[b]	−573.42485	−573.56238	−573.21830	−571.73507	

[a] All distances are in Å and angles in °; MP2 and experimental data are taken from ref.[9] and ref.[14], respectively; the numbering scheme used for **6** is shown in Figure 1.− [b] Total energies in a.u.

tween the planes C1−C4−O/C1−C4−C3−C2 (β) and C1−C4−O/C1−C4−C5−C6 (γ).

Table 2. Calculated geometries and total energies of the isomers *syn*-**2** and *anti*-**2**[a]

Bond or angle	*syn*-**2** B3LYP/ 6-31G*	B3PW91/ 6-31G*	MP2/ 6-31G*	*anti*-**2**[a] B3LYP/ 6-31G*	MP2/ 6-31G*
C1−C2	1.518	1.513	1.508	1.517	1.507
C2−C3	1.343	1.342	1.355	1.337	1.348
C1−C6	1.566	1.560	1.556	1.566	1.555
C5−C6	1.558	1.550	1.549	1.560	1.552
C1−O	1.445	1.437	1.449	1.449	1.452
C1−H	1.090	1.091	1.091	1.090	1.091
C6−H	1.094	1.094	1.093	1.094	1.093
C1−C2−C3	105.7	105.6	105.5	105.9	105.7
C3−C4−C5	108.4	108.2	108.4	106.8	106.5
C1−O−C4	97.0	97.1	96.6	96.8	96.3
H−C6−H	108.1	108.0	108.2	108.5	108.7
β	126.9	126.9	126.6	128.5	128.4
γ	120.2	120.4	120.4	120.2	120.6
H−C1−O−C4	2.2	2.1	3.9	5.2	4.7
Φ	15.8	15.8	17.3	0.0	0.0
E_{tot}[b]	−538.64308	−538.45648	−536.95394	−538.64077	−536.95053

[a] All distances are in Å and angles in°; the numbering schemes used for *syn*-**2** and *anti*-**2** are shown in Figure 1. − [b] Total energies in a.u.

Comparison of the calculated structural parameters for *syn*-**2** and *anti*-**2** shows that their geometries are qualitatively similar, apart from at the double bond. As expected, the double bond of the *syn* isomer exhibits strong deviation from planarity, while the *anti* isomer possesses an essentially planar double bond. It is interesting to note that the degree of double-bond bending in *syn*-**2** (17.3° and 15.8°, as calculated by the MP2/6-31G* and B3LYP/6-31G* approaches, respectively) does not differ significantly from that in *syn*-**1** (16.3° and 15.1°, MP2/6-31G* and B3LYP/6-31G*). The small but notable increase in these angles on going from *syn*-**1** to *syn*-**2** (which is encountered at all levels of calculations employed), can be plausibly explained by: (a) involvement of the repulsive interaction between the nonbonding oxygen lone pairs (n_0) and the π system of the double bond, and (b) differences in the hyperconjugative interaction between the σ orbitals associated with the bridge C−O bonds and the double-bond π orbital. It is, perhaps, interesting to mention that the olefinic carbon atoms in *syn*-**1** and *syn*-**2** possess practically the same s character (ca. 31.50% as calculated by NBO[19] analysis from the B3LYP/6-31G* wavefunction), indicating that rehybridization does not contribute to the observed feature. We note in passing that the observed trend is at variance with the predictions of previous STO-3G Hartree-Fock calculations[6], substantiating the importance of electron correlation in describing structural features of molecules with nonplanar double bonds.

Another interesting point is that the calculated bond lengths of the 7-oxanorbornene subsystems in both molecules are in good accordance with X-ray data obtained for various derivatives of 7-oxanorbornene itself.[20] This is particularly the case for the distribution pattern of the carbon−carbon bond lengths, which is indicative of a strong hyperconjugative interaction between the π system of the double bond and the σ orbitals associated with the carbon−carbon bonds C1−C6 and C4−C5 that are allylic to it (Table 2). Both π-σ*- and π*-σ-type orbital interactions could contribute to this effect. Taking as a reference the B3LYP-optimized geometry of 7-oxanorbornane, where such hyperconjugative interaction is not possible, one observes that this type of interaction causes an elongation of the C1−C6/C4−C5 set of bonds by ca. 0.020 A. A similar trend, although less pronounced, can be seen in the lengths of the bridge carbon−oxygen bonds, which, within the same model, are calculated to be longer by ca. 0.01 A than in the saturated 7-oxanorbornane ring.[21]

Good agreement is also found between the calculated and experimentally available bond angles. For instance, the C−O−C bridgehead angle is calculated to be less than 100°, while the X-ray values for substituted 7-oxanorbornenes lie around 95°. The same holds for the angles between double and C−C single bonds, which are considerably compressed compared to the corresponding angles in unstrained olefins. Both of these features are related to the angular strain of the 7-oxanorbornene framework. Another characteristic of the calculated geometries worthy of mention is related to the tilting of the oxygen bridges away from the central double bond. The tilting angles (β − γ) in the X-ray structures of various 7-oxanorbornene derivatives collected in the Cambridge Crystallographic Data Files fall in the range from 4−12° (average value of ca. 10°). Our B3LYP and MP2 calculations predict a tilting angle of 6.7 and 6.4°, respectively, in *syn*-**2**, while the corresponding values for *anti*-**2** are 8.1 and 7.7°. Since the molecular shape (angles) is in general more accurately reproduced than the molecular size (interatomic distances), the calculated tilting angles can be considered as being very close to the true values.

Finally, it should be noted that the *anti* isomer is predicted to be less stable than the *syn* isomer, the difference in energy being more pronounced at the MP2 (3.5 kcal/mol) than at the B3LYP level of theory (1.5 kcal/mol). The observed trend is in accordance with the stability ordering of *syn*-**1** and *anti*-**1**.[9][17] Moreover, the calculated energy difference between the latter two isomers of 2.6 and 1.5 kcal/mol at the MP2 and B3LYP levels, respectively, is very close to that calculated for *syn*-**2** and *anti*-**2**.

Variable-Temperature PE of Lactone 7

Variable-temperature photoelectron spectroscopy has proved to be well-suited for studying the gas-phase thermolysis of β-lactones and the electronic structure of the thus formed olefins.[22] The reaction takes place in the inlet system of the PE spectrometer at low pressure (10−50 Pa) and can be readily monitored at different temperatures. The onset of thermolysis is easily recognized by the appearance of a sharp signal due to CO_2 (13.76 eV)[23], as can be seen in the recorded PE spectra of lactone **7** shown in Figure 1. The relevant vertical ionization energies and the corresponding MO energies of the starting compound and its decomposition products formed at 500 °C are collected in Table 3. The proposed assignment was made by assuming the validity of Koopmans′ approximation.[24] The lowest vertical ionization and the highest MO energies of olefin *syn*-**2** are also included for the sake of comparison.

Figure 1. PE spectra of β-lactone **7** recorded at different temperatures indicating pyrolysis to *anti*-**2**

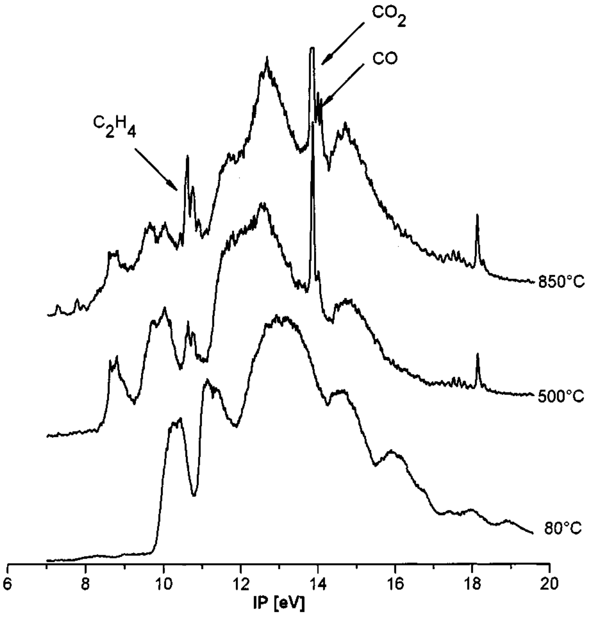

Table 3. First vertical ionization energies ($IE_{v,j}$) and orbital energies (ε_j) calculated by means of HF/6-31G* and HF/STO-3G methods; all values are in eV

Compound	Band	$IE_{v,j}$	Assignment	$-\varepsilon_j$ HF/STO-3G	HF/6-31G*
7	①, ②	10.1	$n_{C=O}$; n^{-}[a]	8.66; 8.87	11.44; 11.66
	③	10.7	n^{-}[b]	9.67	12.33
	②	10.9	n^{+}	9.96	12.34
anti-**2**	①	8.72	44 B_u	7.38	8.96
	②	9.67	43 B_u	8.83	11.16
	③	9.96	42 A_g	9.38	11.78
syn-**2**	①	8.79 [c]	44 A_1	7.50	9.07
	②	9.62	43 B_1	8.83	11.18
	③	10.13	42 A_1	9.46	11.93
	②	10.79	41 B_1	10.48	12.91

[a] With considerable in-phase admixture of the endocyclic oxygen lone-pair orbital of the lactone ring[21]. – [b] With considerable out-of-phase admixture of the $\pi_{C=O}$ of the lactone ring[21]. – [c] Ref.[15].

The PE spectrum in the lowest part of Figure 1 represents that of the starting β-lactone **7**, which appears to be stable up to 400 °C. The spectrum is dominated by two broad bands below 11.5 eV, each of these presumably corresponding to two ionization events. On the basis of comparisons with the calculated MO energies (Table 3), the first feature is associated with ionization from MOs related to the lactone ring, while bands ② and ③ correspond to MOs with predominant contributions from the nonbonding oxygen lone pairs of the ether bridges. Heating of the β-lactone to 500 °C obviously leads to the elimination of CO_2, as indicated earlier. In addition, there are significant changes in the low energy region of the spectrum, the most pronounced of these being the appearance of a new signal at 8.79 eV, and a marked change in the shape and intensity ratio of the first and second ionization bands. The second band is found to be twice as large as the first one. It exhibits two maxima, at 9.67 and 9.96 eV, both of which are at lower ionization energies than the maximum of the first band in the PE spectrum of the starting β-lactone. Additional evidence suggesting that decomposition of the lactone takes place is provided by the pronounced decrease in intensity of the band around 11 eV. Based on comparison of this spectrum with the PE data of the *syn* isomer[15] and the calculated sequence of MO energies (Table 3), we assign the first band to ionization from the π-MO localized predominantly at the central bridge. The measured *IE* is only slightly smaller than in *syn*-**2** (Table 3), in analogy to a trend encountered in comparing the calculated MO energies, as well as the π-*IE*s, of *syn*- and *anti*-sesquinorbornene[25] and of related olefins.[26][27]

Bands ② and ③ appear in the region characteristic for the ionization of nonbonded oxygen lone pair electrons, e.g. in *syn*-**2**[15] and in previously studied 7-oxanorbornene bis adducts.[28][29] They are consequently assigned to the n_O-type orbitals, which within the point group of symmetry C_{2h} transform as B_u and A_g, thus corresponding to the symmetric and antisymmetric linear combinations of the lone pairs, respectively. Their splitting can be understood in terms of the through-bond interaction mechanism.[30][31] It is somewhat smaller than in *syn*-**2** (Table 3), suggesting a less efficacious transfer capability of the intervening σ framework. The experimental trend is fully corroborated by the computational results (Table 3). Finally, the uppermost spectrum shows that increasing the temperature to 850 °C leads to decomposition of the olefin, as evidenced by the appearance of signals for CO (14.03 eV)[23] and ethene (10.56 eV).[23] It is interesting to mention in this regard that decomposition of *anti*-**2** occurs at a lower temperature than for the *syn* isomer[15], in accordance with the calculated difference in their total energies.

Concluding Remarks

Structural and photoelectron-spectroscopic (PES) features of 7,7′-dioxa analogs of *syn*- (*syn*-**2**) and *anti*-sesquinorbornene (*anti*-**2**) have been considered. It is shown that the B3LYP/6-31G* and B3PW91/6-31G* DFT methods are well-suited for studying geometrical properties of large organic molecules containing nonplanar C−C double bonds, as is evident from comparisons with MP2/6-31G* results and available neutron diffraction and X-ray data. The extent of pyramidalization of the double bond carbon atoms in *syn*-**2** is interpreted in terms of π double-bond repulsion with the oxygen lone pairs, its conjugative interaction with the oxygen lone pairs, and its hyperconjugative interaction with the localized σ orbitals of the bridge C−O bonds. It is also shown that the *anti* isomer is less stable than *syn*-**2**, in accordance with the stability ordering of *syn*-**1** and *anti*-**1**. Finally, PES evidence for the formation of *anti*-**2** upon pyrolytic decomposition of the corresponding β-lactone **7** is presented.

Financial support by the *Ministry of Science and Technology of Croatia* (I. A., D. M., Z. B. M. and M. E. M.) and by the *German Federal Ministry of Education, Science, Research, and Technology* is acknowledged.

Experimental Section

General: IR spectra (bands reported in cm^{-1}) were recorded with a Perkin-Elmer M-297 spectrometer. − ^1H- and ^{13}C-NMR spectra were recorded with a JEOL FX90 FT spectrometer in deuteriochloroform solution, with tetramethylsilane (1%) as internal standard. − High-resolution mass spectra (HRMS) were obtained with an EXTREL FTMS 200IDD instrument. − Gas chromatographic analyses were performed using a Varian 3300 gas chromatograph with a DB 15-m column. − Melting points were determined with a Kofler hotplate apparatus and are uncorrected. − The elemental analysis of **7** was performed by the Analytical Service Laboratory of the Rudjer Boskovic Institute.

exo,endo-1,4:5,6-Diepoxy-1,2,3,4,4a,5,6,7,8,8a-decahydronaphthalene-4a,8a-carbolactone (**7**): The lactone was prepared by electrolytic decarboxylation[33] of *exo*,*endo*-1,4:5,8-diepoxy-1,2,3,4,4a,5,6,7,8,8a-decahydronaphthalene-4a,8a-dicarboxylic acid (**8**)[34] according to the procedure described below.

Electrolytic Decarboxylation of **8**: Dicarboxylic acid **8**[34] (1.0 g, 3.9 mmol) was dissolved in 100 ml of 10% aqueous pyridine solution in a cell equipped with two platinum gauze electrodes and a magnetic stirrer. The cell was cooled externally to maintain an internal temperature of 20°C. The cell voltage was continuously increased until the current was approximately 0.8 A. After the electrolysis, the cell contents were separated, and the organic phase was dried with $MgSO_4$ and concentrated under reduced pressure to afford 0.38 g (45%) of a 3:1 mixture of *exo*,*endo*-1,4:5,6-diepoxy-1,2,3,4,4a,5,6,7,8,8a-decahydronaphthalene-4a,8a-carbolactone (**7**) and *exo*,*endo*-1,4:5,6-diepoxy-1,2,3,4,4a,5,6,7,8,8a-decahydronaphthalene-4a,8a-dicarboxylic anhydride. Analytical samples of **7** for use in PE experiments were obtained from the crude product mixture either by sublimation or by column chromatography (silica gel, pentane/ethyl acetate, 2:1); m.p. 129−130°C. − IR (KBr): ν_{max} = 2900 cm^{-1} (aliph. CH), 1820 (C11), 1240 (CH−O−CH), 1040 (C−O). − ^1H NMR ($CDCl_3$): δ = 1.63−2.33 (m, 8 H, 2-H, 3-H, 6-H, 7-H), 4.48 (d, *J* = 5.4 Hz, 1 H), 4.72 (d, *J* = 5.4 Hz, 1 H), 4.79 (t, *J* = 5.3 Hz, 2 H, 1-H, 4-H, 5-H, 8-H). − ^{13}C NMR ($CDCl_3$): δ = 24.30, 24.91, 25.09, 27.70 (4 t, C-2, C-3, C-6, C-7), 74.53, 75.78, 76.54, 78.44 (4 d, C-1, C-4, C-5, C-8), 80.96 (s, C-4a), 90.17 (s, C-8a), 169.17 (s, C-11). − MS; *m*/*z:* 208 [M^+], 164 [$M^+ - CO_2$], 136, 118, 108. − $C_{11}H_{12}O_4$ (208.21): calcd. C 63.46, H 5.77; found C 63.43, H 5.87.

PE Spectroscopy: The PE spectra of **7** were recorded with a Leybold-Heraeus UPG200 spectrometer equipped with a He(I) radiation source (21.21 eV). The spectra were calibrated with the lines of xenon at 12.130 and 13.436 and of argon at 15.759 and 15.937 eV. The accuracy of the measurements was estimated to be approximately ca. 0.03 eV for ionization energies, and ca. 0.1 eV for broad and overlapping signals. The thermolyses were carried out in a heated molybdenum tube 80 mm in length and with an internal diameter of 4.5 mm, which was placed between the sample inlet system and the ionization chamber. The distance between thermolysis tube and ionization chamber was approximately 35 mm. Temperatures are accurate to within ca. ±5°C.

Theoretical Methods: Calculations were carried out using the GAUSSIAN-94 program.[32] The geometry of **6** was fully optimized within the B3LYP formalism employing the 6-31G* and 6-311G* basis sets, and within a framework of the B3PW91/6-31G* model. Calculations on *syn*-**2** were performed at the MP2(fc)/6-31G*, B3LYP/6-31G*, and B3PW91/6-31G* levels of theory, whilst calculations on *anti*-**2** were executed by employing the MP2(fc)/6-31G* and B3LYP/6-31G* methods.

---

[1] [1a] P. D. Bartlett, A. J. Blakeney, M. Kimura, W. H. Watson, *J. Am. Chem. Soc.* **1980**, *102*, 1383−1390. − [1b] W. H. Watson, J. Galloy, P. D. Bartlett, A. A. M. Roof, *J. Am. Chem. Soc.* **1981**, *103*, 2022−2022. − [1c] L. A. Paquette, R. V. C. Carr, M. C. Böhm, R. Gleiter, *J. Am. Chem. Soc.* **1980**, *102*, 1186−1188. − [1d] M. C. Böhm, R. V. C. Carr, R. Gleiter, L. A. Paquette, *J. Am. Chem. Soc.* **1980**, *102*, 7218−7228. − [1e] R. V. Williams, C.-L. A. Sung, H. A. Kurtz, T. M. Harris, *Tetrahedron Lett.* **1988**, 19−20.

[2] For a recent comprehensive review article, see: *Stereochemistry and Reactivity of Systems Containing π-Electrons* (Ed.: W. H. Watson), VCH International, Deerfield Beach, Florida, **1983**.

[3] W. T. Borden, *Chem. Rev.* **1989**, *89*, 1095−1109 and references cited therein.

[4] [4a] K. N. Houk, N. G. Rondan, F. K. Brown, W. L. Jorgensen, J. D. Madura, D. C. Spellmeyer, *J. Am. Chem. Soc.* **1983**, *105*, 5980−5988. − [4b] P. H. Mazzocchi, B. Stahly, J. Dodd, N. G. Rondan, L. N. Domelsmith, M. D. Rozeboom, P. Caramella, K. N. Houk, *J. Am. Chem. Soc.* **1980**, *102*, 6482−6490. − [4c] N. G. Rondan, M. N. Paddon-Row, P. Caramella, K. N. Houk, *J. Am. Chem. Soc.* **1981**, *103*, 2436−2438. − [4d] N. G. Rondan, M. N. Paddon-Row, P. Caramella, J. Mareda, P. H. Mueller, K. N. Houk, *J. Am. Chem. Soc.* **1982**, *104*, 4974−4976.

[5] [5a] R. Gleiter, J. Spanget-Larsen, *Tetrahedron Lett.* **1982**, *23*, 927−930. − [5b] J. Spanget-Larsen, R. Gleiter, *Tetrahedron* **1983**, *39*, 3345−3350.

[6] [6a] J. D. Hagenbuch, P. Vogel, A. A. Pinkerton, D. Schwarzenbach, *Helv. Chim. Acta* **1981**, *64*, 1818−1932. − [6b] P. A. Carrupt, P. Vogel, *J. Mol. Struct. (Theochem.)* **1985**, *124*, 9−23.

[7] P. D. Bartlett, G. L. Combs, *J. Org. Chem.* **1984**, *44*, 625−630.

[8] W. H. Watson, J. Galloy, D. A. Grossie, P. D. Bartlett, G. L. Combs, Jr., *Acta Crystallogr. C* **1984**, *40*, 1050−1054.

[9] M. C. Holthausen, W. Koch, *J. Phys. Chem.* **1993**, *97*, 10021−10027.

[10] W. J. Hehre, L. Radom, D. v. R. Schleyer, J. A. Pople, *Ab initio Molecular Orbital Theory*, Wiley, New York, **1986**.

[11] [11a] T. Ziegler, *Chem. Rev.* **1991**, *91*, 651−667. − [11b] J. K. Labanowski, J. W. Andzelm (Eds.), *Density Functional Methods in Chemistry*, Springer Verlag, New York, **1991**. − [11c] J. M. Seminario, P. Politzer (Eds.), *Modern Density Functional Theory. A Tool for Chemistry in Theoretical and Computational Chemistry*, vol. 2, Elsevier, Amsterdam, **1995**.

[12] [12a] A. D. Becke, *J. Chem. Phys.* **1993**, *98*, 5648−5652. − [12b] C. Lee, W. Yang, R. G. Parr, *Phys. Rev. B* **1988**, *37*, 785−789. − [12c] B. Michlich, A. Savin, H. Stoll, H. Preuss, *Chem. Phys. Lett.* **1989**, *157*, 200−206.

[13] J. P. Perdew, Y. Wang, *Phys. Rev. B* **1992**, *45*, 13244−13249.

[14] O. Ermer, P. Bell, S. A. Mason, *Angew. Chem.* **1989**, *101*, 1298−1301; *Angew. Chem. Int. Ed. Engl.* **1989**, *101*, 1239−1241.

[15] M. Eckert-Maksic, D. Margetic, P. Rademacher, K. Kowski, *Tetrahedron Lett.* **1993**, *34*, 6951−6954.

[16] M. J. Frisch, J. A. Pople, J. S. Binkley, *J. Chem. Phys.* **1984**, *80*, 3265−3269 and references therein.

[17] M. Eckert-Maksic, unpublished results.

[18] [18a] M. Gajhede, F. S. Jorgensen, K. R. Kopecky, W. H. Watson, R. P. Kashyap, *J. Org. Chem.* **1985**, *50*, 4395−4397. − [18b] P. D. Bartlett, G. L. Combs, Jr., A. X. Thi Le, W. H. Watson, J. Galloy, M. Kimura, *J. Am. Chem. Soc.* **1982**, *104*, 3131−3131. − [18c] A. A. Pinkerton, D. Schwarzenbach, J. H. A. Stibbard, P.-A. Carrupt, P. Vogel, *J. Am. Chem. Soc.* **1981**, *103*, 2095−2096. − [18d] L. A. Paquette, A. G. Schaefer, J. F. Blount, *J. Am. Chem. Soc.* **1983**, *105*, 3642−3649. − [18e] L. A. Paquette, P. C. Hayes, P. Charumilind, M. C. Böhm, R. Gleiter, J. F. Blount, *J. Am. Chem. Soc.* **1983**, *105*, 3148−3161.

[19] [19a] J. P. Foster, F. Weinhold, *J. Am. Chem. Soc.* **1980**, *102*, 7211−7218. − [19b] A. E. Reed, L. A. Curtiss, F. Weinhold, *Chem. Rev.* **1988**, *88*, 899−926 and references cited therein.

[20] Cambridge Crystallographic Data File.

[21] M. Eckert-Maksic, N. Novak-Doumbouya, M. Hodoscek, R. Kiralj, B. Kojic-Prodic.

[22] [22a] H. Bock, B. Solouki, *Angew. Chem.* **1981**, 93, 425−442; *Angew. Chem. Int. Ed. Engl.* **1981**, *20*, 427−444 and references cited therein. − [22b] R. Schultz, A. Schweig in *Structure and Reactivity* (Eds.: J. F. Liebman, A. Greenberg), VCH, New York, **1988**, pp. 289−363 and references cited therein.

[23] K. Kimura, S. Katsumata, Y. Achiba, T. Yamazaki, S. Itawa, *Handbook of He(I) Photoelectron Spectra of Fundamental Organic Molecules*, Japan Scientific Societies Press, Tokyo, Halsted Press, New York, **1981**.

[24] T. Koopmans, *Physica* **1934**, *1*, 104−113.

[25] R. S. Brown, J. M. Buschek, K. R. Kopecky, A. J. Miller, *J. Org. Chem.* **1983**, *48*, 3692−3696.

[26] H. Künzer, E. Litterst, R. Gleiter, L. A. Paquette, *J. Org. Chem.* **1987**, *52*, 4740−4744.

[27] M. Bloch, E. Heilbronner, T. B. Jones, J. L. Ripoll, *Heterocycles* **1978**, *11*, 443−453.

[28] [28a] M. Eckert-Maksic, Lj. Maksimovic, *J. Org. Chem.* **1993**, *56*, 3719−3722. − [28b] M. Eckert-Maksic, Lj. Maksimovic, M. Hodoscek, *Tetrahedron Lett.* **1993**, *34*, 4245−4248.

[29] M. Eckert-Maksic, *Photoelectron Spectroscopy of Alcohols, Phenols, Ethers and Peroxides* in *Chemistry of Hydroxyl, Ether and Peroxide Groups*, suppl. E2 (Ed.: S. Patai), Wiley, Chichester, **1993**, pp. 299−371.

[30] [30a] R. Hoffmann, A. Imamura, W. J. Hehre, *J. Am. Chem. Soc.* **1968**, *90*, 1499−1509. − [30b] R. Hoffmann, *Acc. Chem. Res.* **1971**, *4*, 1−9. − [30c] R. Gleiter, *Angew. Chem.* **1974**, *86*, 770−775; *Angew. Chem. Int. Ed. Engl.* **1974**, *13*, 696−741. − [30d] M. N. Paddon-Row, *Acc. Chem. Res.* **1982**, *15*, 245−251.

[31] For a recent review article see: M. Eckert-Maksic in *Theoretical Models of Chemical Bonding*, part 3 (Ed.: Z. B. Maksic), Springer-Verlag, **1991**, pp. 154−198 and references cited therein.

[32] M. J. Frisch, G. W. Trucks, H. B. Schlegel, P. M. W. Gill, B. G. Johnson, M. A. Robb, J. R. Cheeseman, T. Keith, G. A. Peterson, J. A. Montgomery, K. Raghavachari, M. A. Al-Lahan, V. G. Zakrzewski, J. L. Andreas, E. S. Replogle, R. Gomperts, R. L. Martin, D. J. Fox, J. S. Binkley, D. J. Defrees, J. Baker, J. P. Stewart, M. Head-Gordon, C. Gonzalez, J. A. Pople, *GAUSSIAN-94, Revision B.3*, Gaussian Inc., Pittsburg PA, **1995**.

[33] [33a] H. H. Westberg, H. J. Dauben, Jr., *Tetrahedron Lett.* **1968**, 5123−5126. − [33b] R. T. Luibrand, E. M. Fujinari, *J. Org. Chem.* **1980**, *45*, 958−960. − [33c] L. A. Paquette, M. J. Carmody, *J. Am. Chem. Soc.* **1975**, *97*, 5841−5850. − [33d] Lj. Maksimovic, N. Novak, M. Eckert-Maksic, *Synth. Commun.* **1993**, *23*, 3119−3125.

[34] D. Margetic, N. Novak-Doumbouya, M. Eckert-Maksic, to be published.

[98038]